

YOLOv11 Optimization for Efficient Resource Utilization

Areeg Fahad Rasheed¹, M. Zarkoosh²

¹College of Information Engineering, Al-Nahrain University, Baghdad, Iraq
areeg.fahad@coie-nahrain.edu.iq

²Independent Researcher, Baghdad, Iraq
mzarkoosh@gmail.com

Abstract

The objective of this research is to optimize the eleventh iteration of You Only Look Once (YOLOv11) by developing size-specific modified versions of the architecture. These modifications involve pruning unnecessary layers and reconfiguring the main architecture of YOLOv11. Each proposed version is tailored to detect objects of specific size ranges, from small to large. To ensure proper model selection based on dataset characteristics, we introduced an object classifier program. This program identifies the most suitable modified version for a given dataset. The proposed models were evaluated on various datasets and compared with the original YOLOv11 and YOLOv8 models. The experimental results highlight significant improvements in computational resource efficiency, with the proposed models maintaining the accuracy of the original YOLOv11. In some cases, the modified versions outperformed the original model regarding detection performance. Furthermore, the proposed models demonstrated reduced model sizes and faster inference times. Models weights and the object size classifier can be found in this repository ¹.

Keywords: Object detection, YOLOv11, optimization, image size adaptation, scalable detection.

1 Introduction

Object detection is one of the key tasks in computer vision. It represents the ability of a computer model to detect and classify visual objects in images. Object detection is widely used today in various applications

in many fields, such as medicine [3, 24], agriculture [5], industry [20], military [15], etc.

Object detection has evolved through two significant milestones. In the early 1990s, it primarily relied on handcrafted features and sophisticated engineering due to limited image representation techniques [34]. The second era began with the development of convolutional neural networks (CNNs) [11, 14, 25]. However, the adoption of CNNs for object detection was initially delayed due to the lack of access to high-powered computational resources. As advancements in computational capabilities emerged, most object detection techniques in this era began to rely heavily on CNNs [31].

Object detection methods based on convolutional neural networks (CNNs) are typically classified into two types [38, 40]: two-stage object detection and one-stage object detection. In two-stage object detection [8], the algorithm first scans the image to identify regions likely to contain objects using a Region Proposal Network (RPN) [28]. The RPN generates potential regions of interest (ROIs) by assigning an objectness score to each region and refining bounding box proposals. These proposals are then passed to a second stage, where a CNN predicts the object's class and adjusts the bounding box coordinates. Popular algorithms in this category include R-CNN, Fast R-CNN, and Faster R-CNN [28, 6]. This approach is known for its high accuracy and precision but is computationally intensive. In contrast, one-stage object detection skips the region proposal stage and directly predicts the classes and bounding boxes of objects in a single step [39]. This method integrates classification and localization in one unified network, making it faster and more suitable for real-time applications. A prominent example of this type is YOLO (You Only Look Once) [27].

From 2016 to 2024, one-stage object detection methods have gained significantly more popularity and attention from researchers compared to two-stage methods. As illustrated in Figure 1, we analyzed data

¹<https://github.com/AREEG94FAHAD/yolov11>

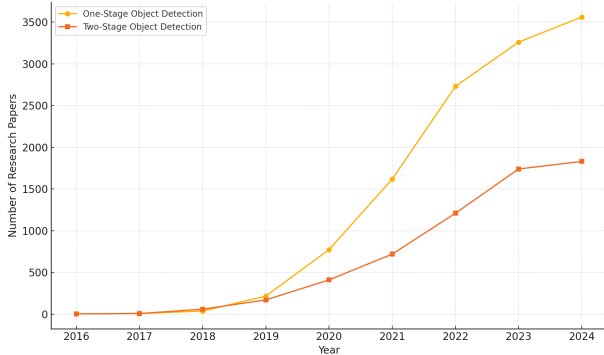


Figure 1: Showing the research trends for one-stage and two-stage object detection methods from 2016 to 2024.

from Google Scholar, collecting information on the number of research papers referencing one-stage and two-stage object detection during this period.

In this paper, we focus on a popular one-stage algorithm, YOLO, specifically version 11, which was developed in 2024 [33, 19]. The main aim of this study is to propose six modified versions of YOLOv11, optimized for computational resources while maintaining the model’s accuracy compared to the original version. Each version is designed to target specific object sizes. This paper can be considered as the YOLOv11 version of the paper [26].

Contributions

1. We proposed six modified versions of YOLOv11, targeting different object sizes. These models are based on modified YOLOv11 and are named as follows: YOLOv11-small, YOLOv11-medium, YOLOv11-large, YOLOv11-sm, YOLOv11-ml, and YOLOv11-sl.
2. Each proposed model has been tested and evaluated on a relevant dataset. The dataset was selected based on an object classification program, and the results were evaluated using standard object detection metrics. The performance of the modified models was compared with the original YOLOv11 model and YOLOv8.

The rest of the paper is organized as follows: In Section II, we provide an overview of the YOLOv11 model and its main components. In Section III, we detail the proposed models. In Section IV, we describe the program used to classify the nature of the dataset and the dataset used to evaluate the models. In Section V, we present the main results and comparisons with recent works. In Section VI, we discuss the limitations of the work and suggest future directions. Finally, in the last section, we conclude by summarizing the key findings.

2 YOLOv11 Overview

YOLO, created by Joseph Redmon et al, in [27], is one of the prominent methods used for object detection. It is based on a one-stage approach, which processes the entire image in a single pass to predict bounding boxes and class probabilities [17]. YOLO has undergone significant development, evolving from its first version to the latest (i.e., YOLOv11) version created by Ultralytics.

YOLOv11 is the latest version of the YOLO family, offering significant improvements in speed, accuracy, and feature extraction. The architecture of YOLOv11, shown in Figure 2, highlights the main components of the model. It generally consists of three key components: the backbone, the neck, and the head. Below, we briefly illustrate each component and the features added to enhance the overall structure.

Backbone: The first main component of YOLOv11 is the backbone, which is responsible for extracting key features at different scales from the input image. This component consists of multiple convolutional (Conv) blocks, each containing three sub-blocks, as shown in Figure 2(b): Conv2D, Batch-Norm2D, and the SiLU activation function. In addition to the Conv blocks, YOLOv11 includes multiple C3K2 blocks, which replace the C2f blocks used in YOLOv8 [13]. The C3K2 blocks provide a more computationally efficient implementation of Cross-Stage Partial (CSP) [35], as illustrated in Figure 2(e). The final two blocks of the backbone are the Spatial Pyramid Pooling Fast (SPPF) and the Cross-Stage Partial with Spatial Attention (C2PSA) [16, 19]. The SPPF block utilizes multiple max-pooling layers, as shown in Figure 2(f), to extract multi-scale features from the input image efficiently. On the other hand, the C2PSA block incorporates an attention mechanism as shown in figure 2 (g), to enhance the model’s accuracy.

Neck: The second main component of YOLOv11 is the neck. As shown in Figure 2, the neck consists of multiple Conv layers, C3K2 blocks, Concat operations, and upsample blocks, along with the advantages of the C2PSA mechanism. The primary role of the neck is to aggregate features at different scales and pass them to the head blocks [13].

Head: The final component of YOLOv11 is the head, a crucial module responsible for generating predictions. It determines the object class, calculates the objectness score, and accurately predicts the bounding boxes for identified objects [18].

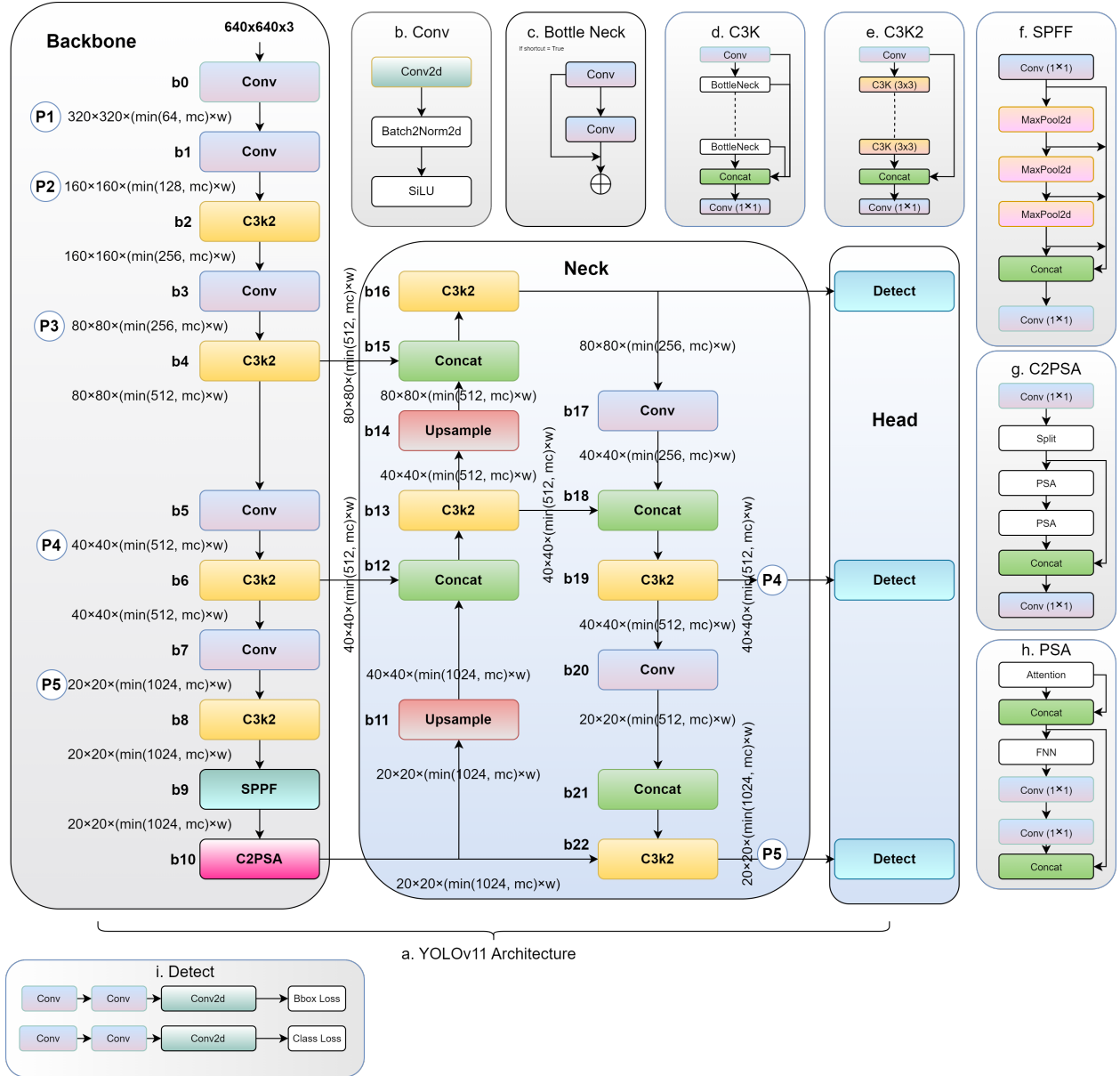


Figure 2: YOLOv11 architecture

3 Modified Versions of YOLOv11

The backbone of the YOLOv11 architecture performs multiple down-sampling operations on the input image, reducing it to scales of 2x, 4x, 8x, 16x, and 32x. This process generates five sets of features (320x320, 160x160, 80x80, 40x40, and 20x20). These feature sets which are named as (P1, P2, P3, P4, P5) see figure 2, are combined with other components of the model, such as SPPF and C2PSA, and then fed into the head blocks. The larger feature sets are responsible for detecting large objects, while the medium-sized feature sets, such as 40x40, are used to detect medium objects. The smallest feature sets, such as 20x20, focus on detecting small objects [4, 10].

According to the official documentation, the YOLOv11 model’s head contains three detection blocks, each responsible for detecting objects of specific sizes. For example, small objects are typically those with a size less than 32^2 pixels, medium objects are those with a size greater than 32^2 but less than 96^2 pixels, and large objects are those with a size exceeding 96^2 pixels [32].

In some cases, object detection applications are designed to focus on specific object sizes. For instance, aerial applications typically involve detecting small objects in images [36, 23]. To enhance resource efficiency, instead of using the standard YOLOv11 architecture, we propose six modified versions of YOLOv11 tailored to detect specific object sizes. (YOLOv11-small, YOLOv11-medium, YOLOv11-large, YOLOv11-sm, YOLOv11-ml, and YOLOv11-sl). Each model targets a specific object size, and the appropriate model is selected based on the datasets’ objects size see Table 1.

To streamline this process, we used a simple program to analyze and provide detailed information about the object sizes in the dataset ², as discussed in the dataset section. Using these modified versions of YOLOv11 instead of the original architecture reduces the computational cost and model size while maintaining accuracy in most scenarios.

In the following sections, we present each proposed modification of YOLOv11 and highlight the main differences between these models and the original architecture.

3.1 YOLOv11-small

The first modified version of YOLOv11 is the small version, which is designed to detect objects with an area less than or equal to 32^2 . To modify YOLOv11,

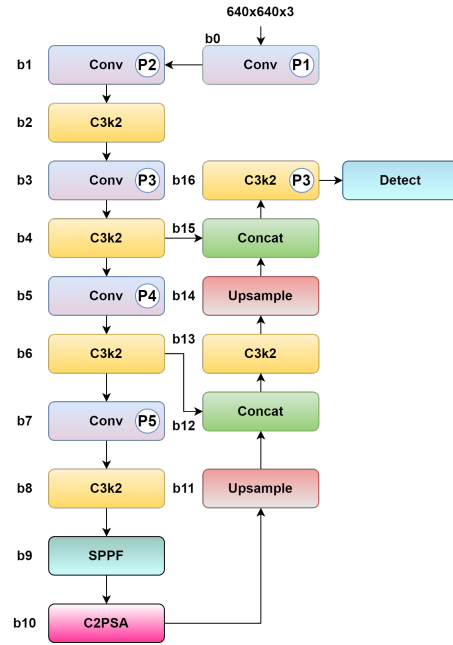


Figure 3: YOLOv11-Small: Architecture Optimized for Detecting Small Objects

we have labeled each block of the original architecture starting with "b," ranging from b0 to b22 for simplicity. As mentioned in the previous section, the first detection head is used for detecting small object sizes [4, 10]. For this, we removed the second and third detection blocks. Since we removed these two detection blocks, we also eliminated the blocks that fed them with features important for detecting larger sizes. As a result, the blocks from b17 to b22, which are related to medium and large objects, were removed. The new version of YOLOv11, called YOLOv11-small, is shown in Figure 3 .

3.2 YOLOv11-medium

The second modified version of YOLOv11 that we proposed specifically targets medium-sized objects, defined as those with sizes greater than 32^2 and less than 96^2 . Back to Figure 2, we removed all blocks related to detecting small and large objects. We eliminated the blocks responsible for processing features related to small and large object detection. Specifically, blocks b14, b15, and b16 were removed as they feed detection heads for small objects [4, 10]. Similarly, blocks b20, b21, and b22 were removed as they feed detection heads for large objects. After removing these blocks, we renamed the original YOLOv11 blocks associated with medium-sized objects (previously b17, b18, and b19) to b14, b15, and b16, respectively, as shown in Figure 4.

²<https://github.com/AREEG94FAHAD/yolov11>

Table 1: Object Size Categories for Modified YOLOv11 Models. Each model is optimized to detect specific object sizes based on the relative area to the image.

Model Name	Object Size Range
YOLOv11-small	$\text{area} \leq 32^2$
YOLOv11-medium	$32^2 < \text{area} \leq 96^2$
YOLOv11-large	$\text{area} > 96^2$
YOLOv11-sm	$\text{area} \leq 96^2$
YOLOv11-ml	$32^2 < \text{area}$
YOLOv11-sl	$\text{area} \leq 32^2$ or $\text{area} > 96^2$

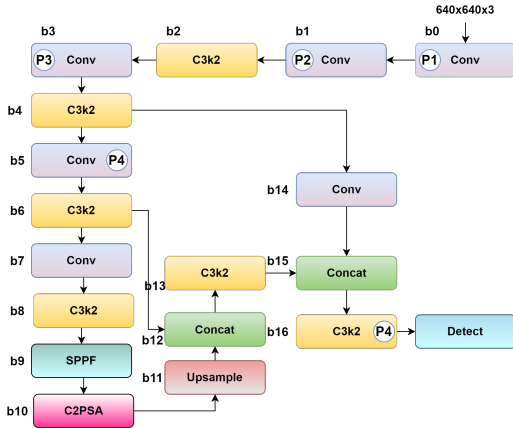


Figure 4: YOLOv11-Medium: Architecture Optimized for Detecting Medium Objects

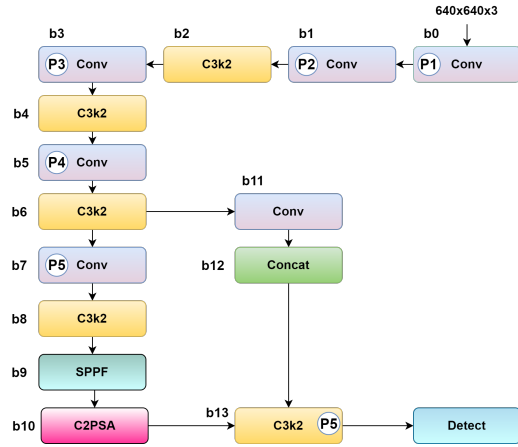


Figure 5: YOLOv11-Large: Architecture Optimized for Detecting Large Objects

3.3 YOLOv11-large

The third modified version of YOLOv11 is designed to target large objects, where the object size area is greater than 96^2 . To create the YOLOv11-large model, modifications were made to the original architecture by removing components unrelated to large object detection and reconnecting previously unlinked blocks [4, 10]. Specifically, blocks b_{11} to b_{19} were removed, as they are associated with providing features for detecting small and medium-sized objects. To ensure continuity in the network, block b_{19} was reconnected to receive features from block b_6 , as both utilize the same feature map as input. Additionally, blocks b_{19} , b_{21} , and b_{22} were renamed to b_{11} , b_{12} , and b_{13} , respectively. The updated architecture of YOLOv11 for large objects is shown in Figure 5.

3.4 YOLOv11-sm

The fourth modified version of YOLOv11, named YOLOv11-sm, is specifically designed to provide flexibility for detecting small and medium-sized objects, where object size areas are less than 96^2 , as shown in Table 1. To implement this modified version, the blocks related to large object detection were removed,

while the blocks for small and medium object detection were remained [4, 10]. As illustrated in Figure 2, the modification involves removing the third detection head and all the blocks that feed into it. Blocks b_{20} , b_{21} , and b_{22} were removed, while the blocks from b_0 to b_{19} remained unchanged. The updated architecture for small and medium object detection in YOLOv11-sm is depicted in Figure 6.

3.5 YOLOv11-ml

The fifth modified version of YOLOv11, referred to as YOLOv11-ml, is designed to target medium and large objects, with object sizes greater than 32^2 . This means that any object exceeding this area can be effectively processed using this model. To derive YOLOv11-ml, modifications were made to the blocks related exclusively to small object detection. Specifically, as shown in Figure 2, blocks b_{14} , b_{15} , and b_{16} were removed. Subsequently, the remaining blocks, b_{17} to b_{22} , were renumbered as b_{14} to b_{19} . Finally block number b_4 linked with block b_{14} . The updated architecture for medium and large object detection is presented in Figure 7.

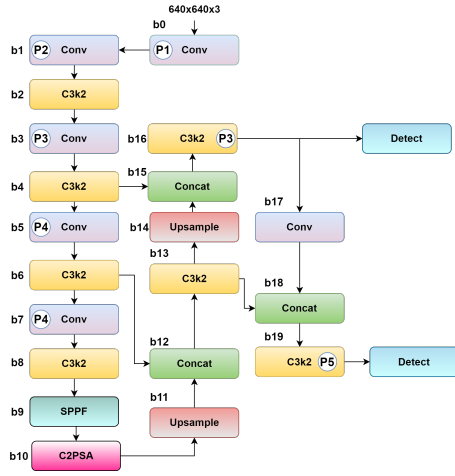


Figure 6: YOLOv11-sm: Architecture Optimized for Detecting small and medium Objects

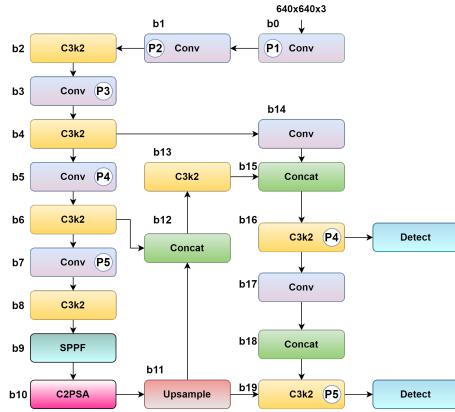


Figure 7: YOLOv11-sm: Architecture Optimized for Detecting medium and large Objects

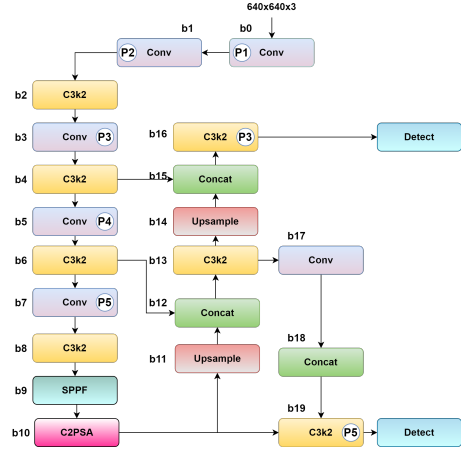


Figure 8: YOLOv11-sl: Architecture Optimized for Detecting small and large Objects

3.6 YOLOv11-sl

The sixth proposed modified version of YOLOv11, referred to as YOLOv11-sl, targets objects that are either small or large, as defined in Table 1, where the object size must satisfy $\text{area} \leq 32^2$ or $\text{area} > 96^2$. To implement this model based on YOLOv11, the blocks related to medium-sized object detection were removed. Specifically, blocks b_{17} , b_{18} , and b_{19} were eliminated, and block b_{20} was reconnected to replace block b_{17} . The numbering of blocks was subsequently adjusted: blocks b_0 to b_{16} remained unchanged, while blocks b_{20} , b_{21} , and b_{22} were renumbered to b_{17} , b_{18} , and b_{19} , respectively. The architecture of this modified version is shown in Figure 8.

4 Datasets Used and Object Size Classification Program

We utilized six different datasets to evaluate the performance of the proposed models. These datasets were sourced from various environments, such as agriculture, medical fields, and others. In addition to the datasets, we also provide details of the program used for classifying the object sizes within the datasets to select the appropriate model for each scenario.

4.1 Object size classifier

As mentioned in the previous section, we proposed six modified versions of YOLOv11, each targeting different object sizes, as shown in Table 1. To select the appropriate model for training, it is essential to understand the nature of the dataset being used. For this purpose, we developed a simple program that processes the training set of the dataset and estimates

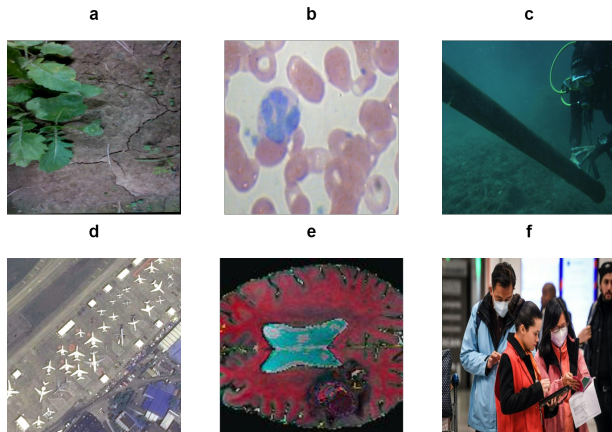


Figure 9: Representative samples from the datasets used — (a) WeedCrop, (b) BCCD, (c) Underwater Pipes, (d) Aerial Airplanes, (e) Brain Tumors, and (f) Face Detection.

the area of all object sizes. Based on these measurements, the program helps select the most suitable model.

The program workflow is as follows: it prompts the user to select the training label directory, iterates through all label files, and computes the size of each object. Each object size is then compared with the predefined size ranges specified in Table 1. If an object instance is classified as small, the program increments the count for small objects, and similarly for other size categories. This process is repeated for all object instances across the dataset. Table 2 presents the object sizes for each dataset discussed in Section 4.2, along with the number of object instances corresponding to each size category.

4.2 Dataset used

The following is a brief description of each dataset used in this paper for the model evaluation process. Figure 9 shows sample form each used dataset.

- WeedCrop [30, 37]: This dataset is used to detect and classify weeds and crops in the agricultural field. All objects in this dataset are categorized into two classes: weed or crop. It comprises 1,176 images containing approximately 7,853 objects. Augmentations such as rotations, shearing, and brightness adjustments were applied to expand the dataset, increasing the total number of objects to 18,693. According to Table 2, most object instances in this dataset are categorized as small-sized. Therefore, this dataset will be used in the following section to evaluate the YOLOv11-small model.

- BCCD [29, 21]: The BCCD dataset is the second dataset used for classifying blood cells. It comprises 364 images with approximately 4,888 objects, commonly used in the medical field. The objects belong to three main classes: 'Platelets,' 'RBC,' and 'WBC.' Augmentation techniques, including flips, rotations, cropping, and adjustments to hue, saturation, brightness, and exposure, expanded the dataset to 874 images with a total of 11,780 objects. As shown in Table 2, approximately 86% of all object instances in the BCCD dataset are classified as medium-sized according to Table 1. Therefore, this dataset will be used to evaluate the medium variant of YOLOv11 (i.e., YOLOv11-medium).
- Underwater pipes [7, 2]: The underwater pipes dataset is used for detecting pipes in underwater environments. It consists of a single class and contains a total of 7,971 images, with 12,238 object instances across the entire dataset. The large modified version of YOLOv11 will be used for this dataset, as the majority of object instances, approximately 96% of the total objects, are classified as large, see Table 2.
- Aerial Airport [7, 12]: The Aerial Airport dataset is used for detecting airplanes in aerial environments. It consists of 338 images with 5,084 object instances. Augmentation techniques, including flips, cropping, and adjustments to hue, saturation, brightness, and exposure, expanded the dataset to 810 images with 11,731 object instances. The appropriate model for this dataset is YOLOv11-sm, as indicated in Table 2, where most object instances in the images belong to the small and medium-sized categories.
- Brain Tumor [1, 22]: The primary purpose of this dataset is to detect brain tumors. It comprises 9,900 images categorized into three classes. Across all splits—training, testing, and validation—the dataset contains a total of 21,888 object instances. Approximately 95% of the object instances in the Brain Tumor dataset fall within the medium and large size ranges, as shown in Tables 1 and 2. Therefore, the YOLOv11-sm modified version is used for the evaluation process of this dataset.
- Face Detection [9]: The final dataset used in this paper is the Face Detection dataset, which consists of 389 images, each containing multiple face instances. The model used for this dataset is YOLOv11-sl, designed for both small and large

Table 2: Dataset Characteristics and the Proper Models for Evaluation

Dataset Name	Total Objects	Small	Medium	Large	Model Used
WeedCrop [30, 37]	18,693	15,237	3,363	93	YOLOv11-small
BCCD [29, 21]	11,780	547	10,094	1,139	YOLOv11-medium
Underwater Pipes [7, 2]	12,238	4	551	11,683	YOLOv11-large
Aerial Airport [7, 12]	11,731	9,008	2,682	41	YOLOv11-sm
Brain Tumor [1, 22]	21,526	1,056	3,484	16,985	YOLOv11-ml
Face Detection	620	21	0	599	YOLOv11-sl

objects, as most object instances in the dataset fall within these two size ranges.

5 Evaluation of Modified YOLOv11 Models

In this section, we present the performance of the proposed models and compare their results with the original YOLOv11 and YOLOv8 models. The main configurations parameters are present in Table 3. The evaluation is divided into two main groups:

- 1- Accuracy and Detection Metrics: This group evaluates performance in terms of recall, precision, and mAP@50.
- 2- Model Efficiency and Resource Utilization: This group focuses on model size, power consumption, inference time.

Table 3: Model Configuration Parameters

Parameter	Value
Epochs	150
Seed	0
Batch Size	16
Weight Decay	0.0005
Patience	100
Learning Rate	0.01

5.1 Accuracy and Detection Metrics

In this section, we evaluate the model performance using metrics such as Recall, Precision, mAP@50. Three models have been used for the evaluation: the first is the YOLOv11 model, the second is a modified version, and the third is the YOLOv8. Each dataset was tested with each model, resulting in a total of 18 experiments.

As shown in Table 4, in most scenarios, the YOLOv11 and the modified version of YOLOv11 outperforms YOLOv8 across all computed metrics, including Recall, Precision, and mAP@50. However, the performance improvement generally does

not exceed 5%. An exception is observed in the BCCD dataset, where YOLOv8 achieves slightly better performance, but the margin is less than 1%. Regarding the performance of the original model (YOLOv11) and the proposed modified models, the results indicate that there is no significant difference in their performance. In four cases, the modified models outperform YOLOv11, as shown in the table. Specifically, YOLOv11-small, YOLOv11-large, YOLOv11-sm, and YOLOv11-sl demonstrate better performance in terms of mAP@50. Conversely, the original YOLOv11 outperforms the modified versions (YOLOv11-medium and YOLOv11-sm). Despite these variations, the maximum performance difference across all metrics is less than 2%.

5.2 Model Efficiency and Resource Utilization

This section presents the performance of the modified models compared to YOLOv8 and YOLOv11 in terms of model size, GFLOPs, inference time, power consumption.

Figure 10 illustrates the sizes of the models (weights and biases) required for deployment on devices. The modified versions of YOLOv11 demonstrate significant improvements in reducing model size. As shown, all the proposed modified versions are smaller than the original YOLOv11 model. Additionally, the results indicate that YOLOv11, with a size of 5.5, is more compact compared to YOLOv8, which has a size of 6.3.

Regarding GFLOPs, which measures the abbreviation measures of giga floating-point operations per second, the results indicate that YOLOv8 requires higher GFLOPs compared to other models see Figure 11. In contrast, YOLOv11 and the proposed modified versions demonstrate better efficiency. When comparing YOLOv11 to its modified versions, the results highlight a substantial reduction in GFLOPs for the modified versions.

The average inference time highlights the better performance of the proposed modified versions of YOLOv11 compared to the original YOLOv11 and YOLOv8. As shown in Figure 12, the inference time

Table 4: Performance comparison of YOLOv11, proposed versions, and YOLOv8 across various datasets.

Dataset	Model	Recall (%)	Precision(%)	mAP@50(%)
WeedCrop[30, 37]	YOLOv11	67.07	70.62	69.09
	YOLOv11-small	70.98	69.27	69.27
	YOLOv8	63.98	63.98	68.50
BCCD[29, 21]	YOLOv11	91.95	84.90	92.98
	YOLOv11-medium	90.56	85.34	92.67
	YOLOv8	91.62	86.93	93.19
Underwater Pipes[7, 2]	YOLOv11	99.15	99.01	99.43
	YOLOv11-large	98.90	99.21	99.48
	YOLOv8	99.46	98.60	99.47
Aerial Airport[7, 12]	YOLOv11	87.42	91.73	92.93
	YOLOv11-sm	86.91	93.15	93.20
	YOLOv8	87.05	90.87	92.23
Brain Tumor[1, 22]	YOLOv11	74.73	89.21	81.67
	YOLOv11-ml	72.05	90.90	80.15
	YOLOv8	72.46	90.80	80.49
Face Detection[9]	YOLOv11	93.10	97.98	96.14
	YOLOv11-sl	93.10	93.05	97.70
	YOLOv8	87.93	93.63	93.05

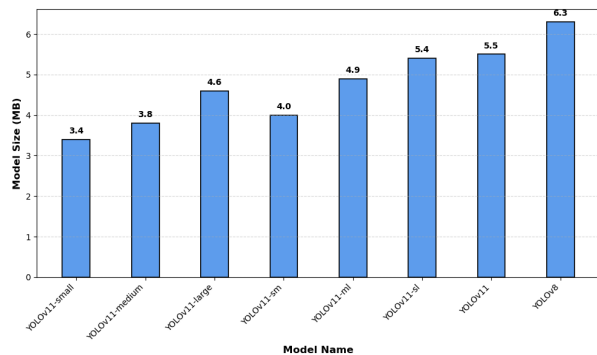


Figure 10: Model Size (MB)

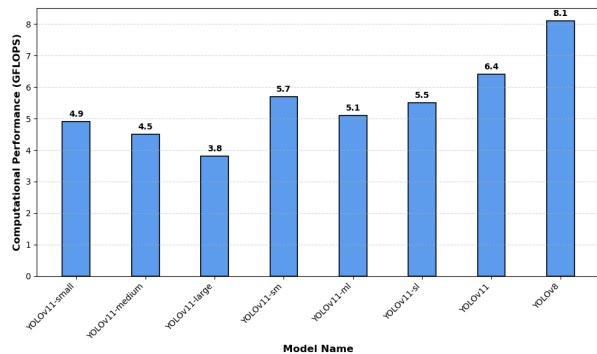


Figure 11: Computational Performance (GFLOPS)

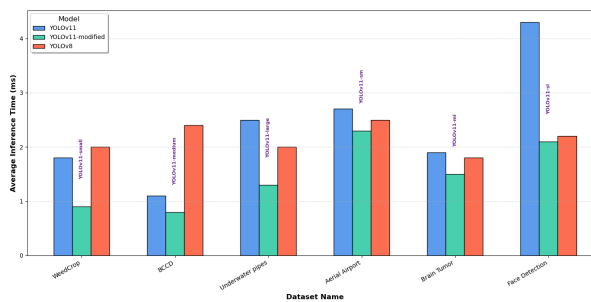


Figure 12: Average Inference Time per Image (ms)

of the modified versions is consistently lower across all scenarios. Additionally, all versions, including the original models, achieved an inference time of less than 5 milliseconds. The difference in inference time across all models for the same dataset is approximately 2 milliseconds.

Figure 13 illustrates the power consumption results for each model, calculated per epoch. As shown, four of the proposed models (YOLOv11-small, YOLOv11-medium, YOLOv11-large, and YOLOv11-ml) outperform the original YOLOv11 and YOLOv8 in terms of power efficiency. Meanwhile, YOLOv11-sm and YOLOv11-sl demonstrate performance comparable to the other models.

6 Discussion

The following the key points discussed regarding the results and how the proposed models improve perfor-

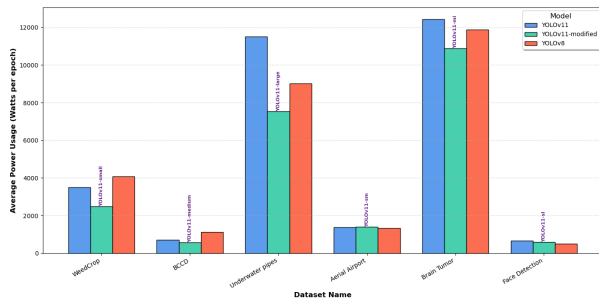


Figure 13: Average Power Usage (Watts per epoch)

mance:

- 1- **Maintaining Accuracy:** The proposed models were designed by removing specific blocks that do not contribute to detecting particular object sizes based on the dataset. This strategic removal of unrelated blocks has a minor impact on accuracy and, in some cases, even enhances it. For example, YOLOv11-small and YOLOv11-large perform better than the original model.
- 2- **Reduction in Model Size:** By eliminating blocks unrelated to specific object size, the proposed models achieved size reduction. Furthermore, removing blocks associated with other object sizes contributed to additional reductions. For instance, the size of YOLOv11-sm decreased to 4 MB, and further removal of medium object-related blocks reduced it to 3.4 MB.
- 3- **Reduction in GFLOPS:** Removing blocks feeding the detection head that are unrelated to specific object sizes not only improved performance but also reduced the number of operations required. For example, removing both medium and large object-related components resulted in a high reduction in GFLOPS, as observed in models like YOLOv11-small.
- 4- **Inference Time:** Minimizing the YOLOv11 architecture resulted in a reduced number of operations required for processing, thereby decreasing the inference time. As shown in the results, all the proposed models achieved lower inference times compared to the original YOLOv11 and YOLOv8.
- 5- **Power Usage:** The results indicate that reducing the model architecture decreases power consumption during training. As shown, YOLOv11-small, YOLOv11-medium, YOLOv11-large, and YOLOv11-ml achieved lower power consumption compared to both the original YOLOv11 and YOLOv8. Meanwhile, YOLOv11-sm

and YOLOv11-sl demonstrated approximately the same power consumption as the original YOLOv11 and YOLOv8.

7 Limitation and Future works

Although the proposed modified versions of YOLOv11 performed well in most performance metrics, such as power consumption, reduction of model size, inference time, and computational efficiency, their suitability depends on the target application. For instance, in medical applications where object sizes (e.g., cells) remain constant, the modified versions may be ideal. However, for applications involving objects with varying sizes, such as car detection on roads where cars appear larger when closer to the camera and smaller when farther away, using the full version of YOLOv11 might be more effective.

To address such scenarios, we recommend implementing a preprocessing step to classify dataset objects by size using the program which is mentioned in Section 4.1, enabling the selection of the most suitable modified version. In addition, we suggest testing the proposed models in uncontrolled environments, such as foggy conditions.

Furthermore, the current implementation uses 32-bit integers to represent model parameters. We recommend experimenting with different quantization methods to reduce the model size and evaluating the models both before and after applying quantization techniques.

8 Conclusion

This paper presents six modified versions based on the latest YOLOv model, YOLOv11. These modified versions are designed to target the detection of specific object size ranges. Each of the six proposed models focuses on a particular object size category, such as small, medium, large, small-medium, medium-large, and small-large objects.

To select the appropriate model for a given dataset, an analysis of the dataset is required to determine the predominant object sizes. For this purpose, we developed a program to compute and classify object sizes effectively. Each proposed model was tested on different datasets and compared with two other models, YOLOv11 and YOLOv8.

The overall results demonstrate that using the modified versions instead of training on whole model (YOLOv11, or YOLOv8) to detect all object sizes provides better performance. These modified versions also utilize fewer resources compared to the

original YOLOv11 and YOLOv8 models. Despite the reduced resource usage, the accuracy of the modified models did not decrease significantly compared to the original models. In some cases, the modified models even outperformed the original versions. Ultimately, we also mention the main limitations of the work and suggest different areas that can be addressed in the future.

References

- [1] R. 100. brain tumor dataset. <https://universe.roboflow.com/roboflow-100/brain-tumor-m2pbp>, may 2023. visited on 2024-11-27.
- [2] R. 100. underwater pipes dataset. <https://universe.roboflow.com/roboflow-100/underwater-pipes-4ng4t>, may 2023. visited on 2024-11-27.
- [3] H. A. Ahmed and E. A. Mohammed. Detection and classification of the osteoarthritis in knee joint using transfer learning with convolutional neural networks (cnns). *Iraqi Journal of Science*, pages 5058–5071, 2022.
- [4] M. A. R. Alif. Yolov11 for vehicle detection: Advancements, performance, and applications in intelligent transportation systems. *arXiv preprint arXiv:2410.22898*, 2024.
- [5] C. M. Badgular, A. Poulouse, and H. Gan. Agricultural object detection with you only look once (yolo) algorithm: A bibliometric and systematic literature review. *Computers and Electronics in Agriculture*, 223:109090, 2024.
- [6] P. Bharati and A. Pramanik. Deep learning techniques—r-cnn to mask r-cnn: a survey. *Computational Intelligence in Pattern Recognition: Proceedings of CIPR 2019*, pages 657–668, 2020.
- [7] F. Ciaglia, F. S. Zuppichini, P. Guerrie, M. McQuade, and J. Solawetz. Roboflow 100: A rich, multi-domain object detection benchmark. *arXiv preprint arXiv:2211.13523*, 2022.
- [8] L. Du, R. Zhang, and X. Wang. Overview of two-stage object detection algorithms. In *Journal of Physics: Conference Series*, volume 1544, page 012033. IOP Publishing, 2020.
- [9] Facedataset. Face for small large dataset. <https://universe.roboflow.com/ok-4sjtq/face-for-small-large>, may 2024. visited on 2024-11-27.
- [10] F. Feng, Y. Hu, W. Li, and F. Yang. Improved yolov8 algorithms for small object detection in aerial imagery. *Journal of King Saud University-Computer and Information Sciences*, 36(6):102113, 2024.
- [11] K. Fukushima. Neocognitron: A self-organizing neural network model for a mechanism of pattern recognition unaffected by shift in position. *Biological cybernetics*, 36(4):193–202, 1980.
- [12] GDIT. Aerial airport dataset. <https://universe.roboflow.com/gdit/aerial-airport>, may 2024. visited on 2024-11-27.
- [13] A. Ghosh. Yolov11 overview. <https://learnopencv.com/yolo11/>, 2024. Accessed on November 25, 2024.
- [14] J. Gu, Z. Wang, J. Kuen, L. Ma, A. Shahroudy, B. Shuai, T. Liu, X. Wang, G. Wang, J. Cai, et al. Recent advances in convolutional neural networks. *Pattern recognition*, 77:354–377, 2018.
- [15] R. D. Haameid, B. Q. Al-Abudi, and R. N. Hassan. Automatic object detection, labelling, and localization by camera’s drone system. *Iraqi Journal of Science*, pages 5008–5023, 2021.
- [16] K. He, X. Zhang, S. Ren, and J. Sun. Spatial pyramid pooling in deep convolutional networks for visual recognition. *IEEE transactions on pattern analysis and machine intelligence*, 37(9):1904–1916, 2015.
- [17] M. Hussain and R. Khanam. In-depth review of yolov1 to yolov10 variants for enhanced photovoltaic defect detection. In *Solar*, volume 4, pages 351–386. MDPI, 2024.
- [18] N. Jegham, C. Y. Koh, M. Abdelatti, and A. Hendawi. Evaluating the evolution of yolo (you only look once) models: A comprehensive benchmark study of yolo11 and its predecessors. *arXiv preprint arXiv:2411.00201*, 2024.
- [19] R. Khanam and M. Hussain. Yolov11: An overview of the key architectural enhancements. *arXiv preprint arXiv:2410.17725*, 2024.
- [20] R. Khanam, M. Hussain, R. Hill, and P. Allen. A comprehensive review of convolutional neural networks for defect detection in industrial applications. *IEEE Access*, 2024.
- [21] H. Kutlu, E. Avci, and F. Özyurt. White blood cells detection and classification based on regional convolutional neural networks. *Medical hypotheses*, 135:109472, 2020.

- [22] Z. Lin, W. Lin, and F. Jiang. Yolov8-dec: Enhancing brain tumor object detection accuracy in magnetic resonance imaging. *Progress in Electromagnetics Research M*, 129, 2024.
- [23] M. Liu, X. Wang, A. Zhou, X. Fu, Y. Ma, and C. Piao. Uav-yolo: Small object detection on unmanned aerial vehicle perspective. *Sensors*, 20(8):2238, 2020.
- [24] M. G. Ragab, S. J. Abdulkader, A. Muneer, A. Alqushaibi, E. H. Sumiea, R. Qureshi, S. M. Al-Selwi, and H. Alhussian. A comprehensive systematic review of yolo for medical object detection (2018 to 2023). *IEEE Access*, 2024.
- [25] A. F. Rasheed and M. Zarkoosh. Unveiling derivatives in deep and convolutional neural networks: A guide to understanding and optimization. *Authorea Preprints*, 2024.
- [26] A. F. Rasheed and M. Zarkoosh. Optimized yolov8 for multi-scale object detection. *Journal of Real-Time Image Processing*, 22(1):6, 2025.
- [27] J. Redmon. You only look once: Unified, real-time object detection. In *Proceedings of the IEEE conference on computer vision and pattern recognition*, 2016.
- [28] S. Ren, K. He, R. Girshick, and J. Sun. Faster r-cnn: Towards real-time object detection with region proposal networks. *IEEE transactions on pattern analysis and machine intelligence*, 39(6):1137–1149, 2016.
- [29] Roboflow. Bccd dataset. <https://universe.roboflow.com/joseph-nelson/bccd>, aug 2022. visited on 2024-11-27.
- [30] K. Sudars, J. Jasko, I. Namatevs, L. Ozola, and N. Badaukis. Dataset of annotated food crops and weed images for robotic computer vision control. *Data in brief*, 31:105833, 2020.
- [31] N. C. Thompson, K. Greenewald, K. Lee, and G. F. Manso. The computational limits of deep learning. *arXiv preprint arXiv:2007.05558*, 2020.
- [32] Ultralytics. Yolov11 classification of object sizes. <https://github.com/ultralytics/ultralytics/issues/8090>, 2024. Accessed: 2024-11-26.
- [33] Ultralytics. Yolov11 documentation, 2024. Accessed: 2024-11-24.
- [34] P. Viola and M. Jones. Rapid object detection using a boosted cascade of simple features. In *Proceedings of the 2001 IEEE computer society conference on computer vision and pattern recognition. CVPR 2001*, volume 1, pages I–I. Ieee, 2001.
- [35] C.-Y. Wang, A. Bochkovskiy, and H.-Y. M. Liao. Scaled-yolov4: Scaling cross stage partial network. In *Proceedings of the IEEE/cvf conference on computer vision and pattern recognition*, pages 13029–13038, 2021.
- [36] J. Wang, W. Yang, H. Guo, R. Zhang, and G.-S. Xia. Tiny object detection in aerial images. In *2020 25th international conference on pattern recognition (ICPR)*, pages 3791–3798. IEEE, 2021.
- [37] N. Workspace. Weedcrop dataset. <https://universe.roboflow.com/new-workspace-csmgu/weedcrop-waif1>, jul 2022. visited on 2024-11-27.
- [38] X. Wu, D. Sahoo, and S. C. Hoi. Recent advances in deep learning for object detection. *Neurocomputing*, 396:39–64, 2020.
- [39] Y. Zhang, X. Li, F. Wang, B. Wei, and L. Li. A comprehensive review of one-stage networks for object detection. In *2021 IEEE International Conference on Signal Processing, Communications and Computing (ICSPCC)*, pages 1–6. IEEE, 2021.
- [40] Z. Zou, K. Chen, Z. Shi, Y. Guo, and J. Ye. Object detection in 20 years: A survey. *Proceedings of the IEEE*, 111(3):257–276, 2023.